







Superconducting skutterudite-like CeP₃

Xing Li ¹, Aitor Bergara ^{2,3,4,*}, Xiaohua Zhang ¹, Shicong Ding ¹, Yong Liu ¹, and Guochun Yang ^{1,†}

¹State Key Laboratory of Metastable Materials Science & Technology and Key Laboratory for Microstructural Material Physics of Hebei Province, School of Science, Yanshan University, Qinhuangdao 066004, China

²Physics Department and EHU Quantum Center, Universidad del País Vasco-Euskal Herriko Unibertsitatea, UPV/EHU, 48080 Bilbao, Spain

³Donostia International Physics Center (DIPC), 20018 Donostia, Spain

⁴Centro de Física de Materiales CFM, Centro Mixto CSIC-UPV/EHU, 20018 Donostia, Spain



(Received 30 October 2023; accepted 24 January 2024; published 23 February 2024)

The exploration of new pathways to achieve superconductivity in materials has always been a central focus of research in condensed matter physics. Skutterudites have garnered attention due to their intriguing physical properties and broad range of applications. In this study, we propose that rotating the planar P₄ units within skutterudites is a viable method to induce superconductivity. The predicted compound, referred to as skutterudite-like CeP₃, exhibits phonon-mediated superconductivity at ambient pressure. This phenomenon arises from the interaction between Ce/P-derived phonons and the Ce 4*f* and P 3*p* electrons. The energy barrier for transitioning from the skutterudite-like CeP₃ to the conventional skutterudite-type CeP₃ is as high as 1.53 eV/atom, indicating a substantial irreversibility. Additional calculations reveal that skutterudite-like CeP₃ becomes thermodynamically stable at 25 GPa in the binary Ce-P phase diagram. Consequently, the skutterudite-like CeP₃ can be synthesized by initially compressing the most stable bulk binary CeP and P at 25 GPa, followed by decompression. This work represents a significant step forward in the design of superconducting skutterudite-like compounds.

DOI: [10.1103/PhysRevB.109.054522](https://doi.org/10.1103/PhysRevB.109.054522)

I. INTRODUCTION

Skutterudites MX_3 (e.g., $M = \text{Co, Rh, Ir}$; $X = \text{P, As, Sb}$), are materials composed of intricately nested high-symmetry atomic building blocks of metals (M) and pnictogens (X) [1,2], and have attracted significant attention in condensed matter physics and materials science [3]. This interest stems from their diverse and interesting properties, which have led to their classification as multifunctional families, including thermoelectrics [4–6], non-Fermi liquids [7–9], heavy-fermion compounds [10,11], and superconductors [12,13]. Most conventional skutterudites are semiconducting due to their standard stoichiometry, which is unfavorable for the onset of superconductivity [14]. So far, superconductivity in skutterudites has been induced and controlled by introducing additional alkaline-earth metal, transition metal, or lanthanide atoms into the interstitial spaces for electron doping [15,16]. The morphology and distribution of the original M/X atomic building blocks remain unchanged. Moreover, Qi *et al.* made an innovative discovery that a small amount of P/As atoms in IrP₃/IrAs₃ can be self-inserted into the interstitial region for hole doping when subjected to hydrostatic pressure [17], resulting in the achievement of superconductivity. From a different perspective, superconductivity in skutterudites may also be associated with variations in the atomic building blocks (X_4), offering a unique opportunity to explore superconducting compounds.

The design and selection of regulatory pathways to alter the building blocks in compounds have become a promising approach for the development of functional materials. To the best of our knowledge, the technique of rotation has shown significant potential in stabilizing compounds with unique properties [18–25]. For instance, double-layer graphene with a precise torsion angle exhibits astonishing superconductivity [18], reshaping our understanding of the carbon attributes and graphene itself. Pressure-induced K₂ReH₉ undergoes a transition from a semiconductor to a metal and superconductor due to the rotation of the H triangle within its structure [19]. It exhibits remarkable superconductivity at 127.1 K under 75 GPa. Furthermore, oxygen-octahedral rotations are prevalent in perovskite-type compounds, illustrating their effectiveness in modulating stability [20], inducing magnetic transformation [21], achieving negative thermal expansion [22], and controlling magnetic anisotropy [23,24], among other features.

Pressure, as the most powerful method of overcoming reaction barriers, has been extensively used in the synthesis of unknown compounds, particularly those that cannot be obtained at ambient pressure [26,27]. Remarkably, certain pressure-induced compounds can even be quenched and stabilized at ambient pressure [28]. Moreover, numerous compounds exhibit distinct properties linked to their unique structural components [29–32]. For examples, two groundbreaking discoveries, H₃S and LaH₁₀, showcase high-temperature superconductivity attributed to the S-H covalent framework [29] and the sodalite-like hydrogen cage [30], respectively. SrB₃C₃, an exceptionally lightweight and durable material recently synthesized, exhibits both superconductivity

*Corresponding author: a.bergara@ehu.es

†Corresponding author: yanggc468@nenu.edu.cn

and hardness, which can be related to the truncated octahedral BC cage [28,31]. Furthermore, CeH₉, stabilized at much lower pressures (<100 GPa) compared to many polyhydride superconductors, also displays superconductivity primarily driven by the H₂₉ cage [32].

Taking the aforementioned factors into account, we propose an innovative approach to stabilize a different category of skutterudites, referred to as skutterudite-like structures. This method involves manipulating the orientation of the P₄ units within the traditional skutterudite lattice, facilitated by first-principles calculations. Specifically, we have identified 14 dynamically stable compounds that can exist under ambient pressure conditions. Notably, CeP₃, a skutterudite-like compound, demonstrates unexpected superconductivity under ambient pressure. We have also investigated the potential synthesis pathway, which involves the most stable bulk CeP and P to a compression of 25 GPa followed by annealing to return to ambient pressure. Our research introduces a different approach to modulate the superconducting properties of skutterudites.

II. COMPUTATIONAL DETAILS

The structural design of skutterudite-like compounds was accomplished using the three-dimensional visualization software VESTA [33]. We have applied the density functional theory (DFT) for the high-throughput screening, utilizing the Vienna *ab initio* simulation package (VASP) code [34]. Our primary criterion for the evaluation was the dynamical stability of the designed compounds, which we assessed using the PHONOPY code through the supercell finite displacement method [35]. The projector augmented wave (PAW) with $5s^25p^64f^15d^16s^2$ and $3s^23p^3$ electrons are adopted as valence electrons for Ce and P atoms, respectively [36]. The exchange-correlation functional was treated with the Perdew-Burke-Ernzerhof (PBE) generalized gradient approximation [37]. A kinetic cutoff energy of 600 eV was applied, along with the Monkhorst-Pack scheme featuring a k -point grid of $2\pi \times 0.03 \text{ \AA}^{-1}$ in the Brillouin zone, ensuring an enthalpy convergence of less than 1 meV/atom. To estimate the potential barrier for transitioning from the skutterudite-like CeP₃ to the conventional skutterudite-type CeP₃ at ambient pressure, we conducted a variable-cell nudged elastic band (VCNEB) calculation using the USPEX code [38,39]. The electron localization function (ELF) was employed to describe the electron distribution [40] and the nature and strength of the chemical bonding. Furthermore, the crystal orbital Hamilton population (COHP), a more in-depth method for analyzing the origins of chemical bondings, was computed using the LOBSTER package [41]. To assess the electron-phonon coupling (EPC) in skutterudite-like CeP₃, we carried out calculations with the QUANTUM ESPRESSO package based on density functional perturbation theory (DFPT) [42].

III. RESULTS AND DISCUSSION

In conventional skutterudites, the metal atoms (M) are located at 8c sites, creating a simple cubic (sc) sublattice [Fig. 1(a)]. On the other hand, the nonmetal atoms ($X = P, As, Sb$) occupy the 24g sites, forming rectangular planar X_4

rings with edges aligned along the directions of the base vectors. Additionally, these X_4 rings exhibit different orientations along the a , b , and c axes within the plane, giving rise to three distinct types of body centered cubic (bcc) sublattices [2].

Given the substantial interstitial region around the P₄ ring in conventional skutterudite MP_3 , previous studies have demonstrated that the introduction of additional atoms can effectively modulate the properties, such as superconductivity [15,16]. This characteristic presents an opportunity to manipulate the P₄ ring appropriately for the design of novel skutterudite-like structures. In our quest to identify a low-energy configuration, we systematically rotated all P₄ rings uniformly at intervals of 2.5/5 degrees within the range 0–90° around their planar symmetry center [Fig. 1(b)]. We combined this rotation with a transformation of the P₄ ring from a rectangle to a rhombus shape, which alters atomic interactions and results in a more compact structure with lower energy. Notably, when the diagonals of the P₄ ring align with the directions of the basis vectors (approximately a rotation angle of 45°), the corresponding structure exhibits the lowest energy [Fig. 1(c)]. Interestingly, this structure shares the same space group ($Im\bar{3}$) and sc M sublattice as the conventional skutterudite. However, the P₄ ring consists of two nonequivalent P atoms occupying the 12d and 12e sites, named P1 and P2, respectively. Additionally, the distances between the M atoms and P1/P2 atoms are extended, while the distances between the M atoms, as well as the lattice constants, are shortened. These characteristics favor a reduction in the total energy, as will be discussed later.

It is well established that the crystal structure of a compound plays a pivotal role in determining its properties. Therefore, the variations in interatomic distances and atomic distribution inevitably lead to differences in chemical bonding and electronic properties. Additionally, within the same structural configuration, the use of different metal elements with distinct attributes can also result in property variations. Consequently, based on the proposed rotated skutterudite-like structure, we conducted a comprehensive high-throughput screening involving third-, fourth-, and fifth-row transition elements, as well as lanthanoid elements from the Periodic Table [Fig. 1(d)]. As anticipated, we have identified 14 previously unknown compounds that maintain their dynamic stability at ambient pressure, including compounds like YP₃, LaP₃, and CeP₃ [Fig. 1(d) and Fig. S1 of the Supplemental Material [43]] [41,42,44–49]. For these compounds, we observed that as the atomic number increases, the lattice constant and the distance of M -P1/P2 interactions initially increase (from Y to La) and then gradually decrease and converge (Fig. 2). The former can be attributed to the increase in the atomic radius, while the latter is due to the contraction effect of $4f$ electrons. Additionally, Bader charge analysis indicates that the amount of charge transfer gradually decreases and tends to converge with the increasing atomic number. More intriguingly, for Y and La elements, which lack $4f$ electrons (Fig. 2), their compounds are indirect band-gap semiconductors with band-gap value of 0.13 and 0.07 eV, respectively (Fig. S2 [43]). In contrast, compounds with elements possessing $4f$ electrons display metallic behavior, distinct from the semiconducting nature of most conventional skutterudites. Furthermore, their electronic density of states (DOS) at the

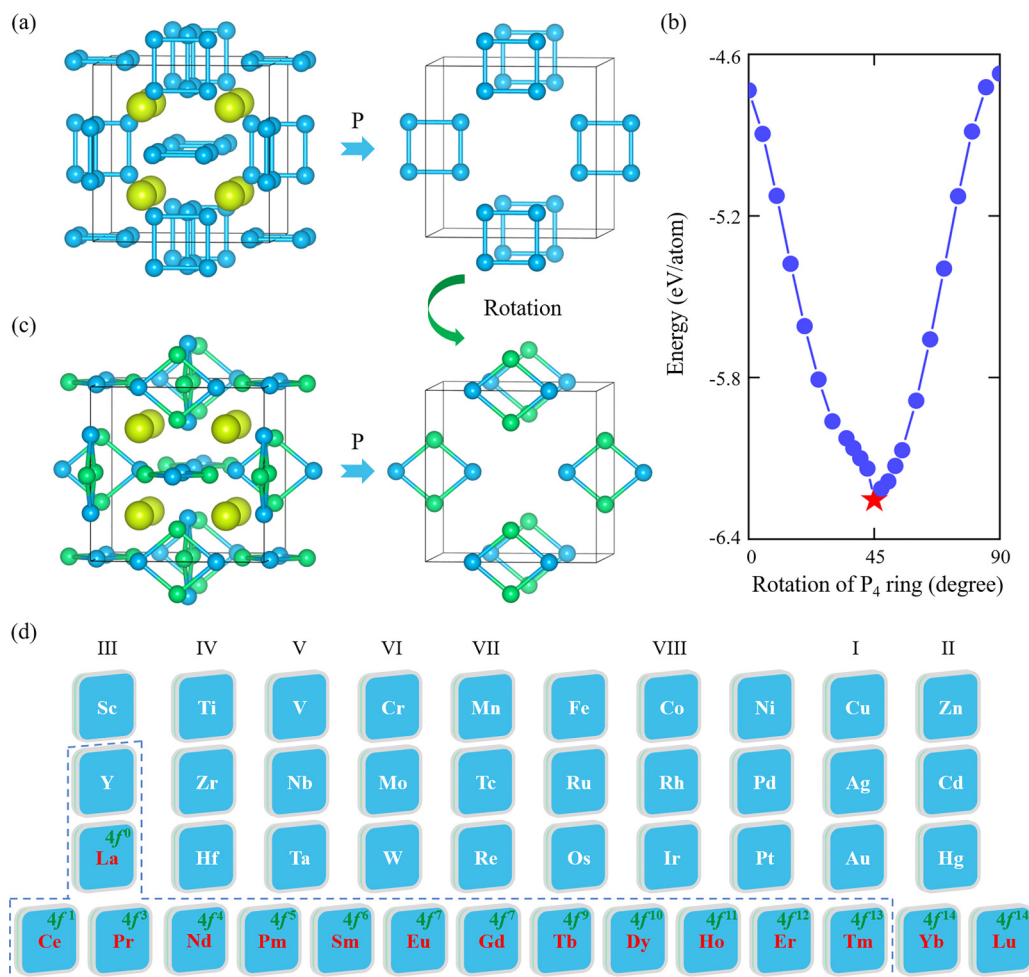


FIG. 1. (a) Crystal structure and P atomic building block of the conventional skutterudite MP_3 . (b) The total energy as a function of the rotation of the P_4 rings in conventional skutterudite-type MP_3 ($M = Ce$). (c) Crystal structure and P_4 units of the designed skutterudite-like MP_3 . For clarity, the yellow sphere represents a M atom, and the blue and green spheres represent nonequivalent P_1 and P_2 atoms. (d) The considered elements used to explore the skutterudite-like MP_3 compounds in the periodic table. The corresponding rotated skutterudite-like compounds of the elements in the dashed box are stable, while the others are unstable. In addition, for red lanthanoid elements, the number of electrons in their $4f$ orbitals is shown in green in the upper right corner of the element box.

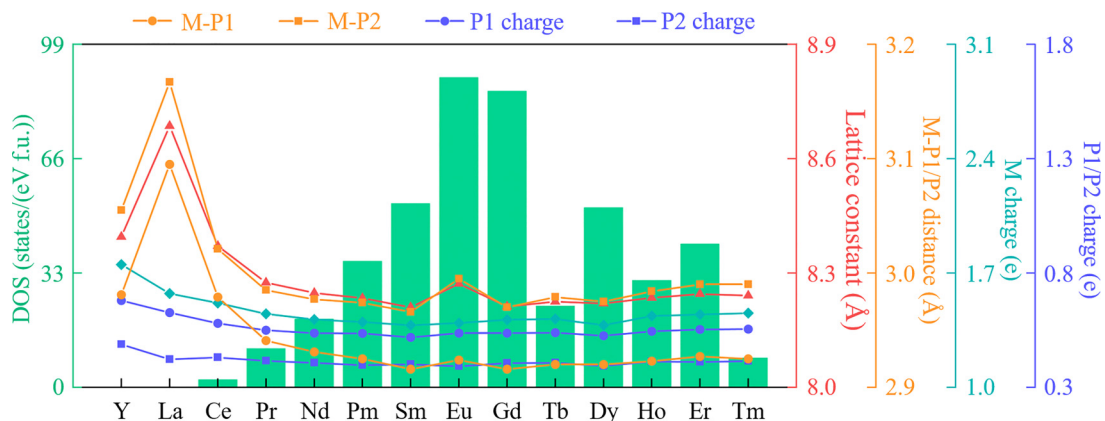


FIG. 2. The lattice constants, the distances of the M - P_1 / P_2 interactions, the donated/accepted charge amount of the M / P_1 / P_2 atom, and the DOS of the stable rotated skutterudite-like compounds at ambient pressure.

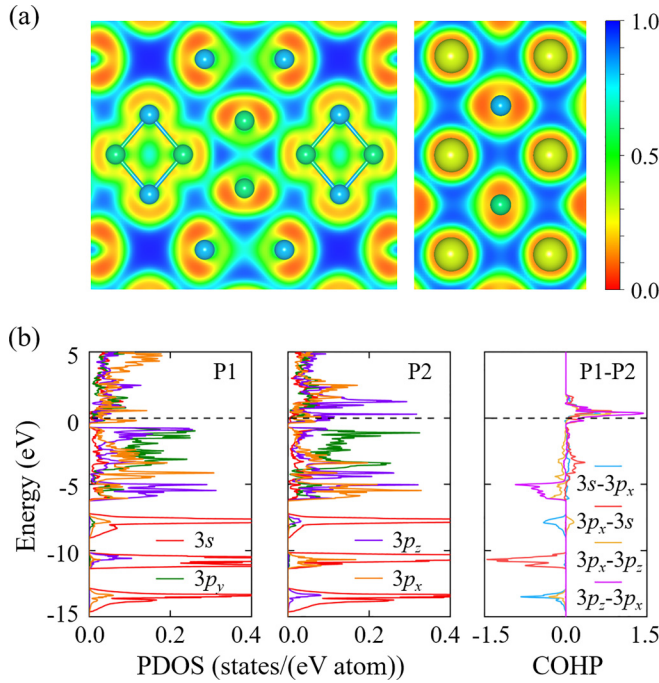


FIG. 3. (a) The ELF maps in two parallel (0 1 0) planes with different atomic arrangements. (b) The orbital-resolved PDOS of P1 and P2 atoms, and the COHP of the P1-P2 interaction in skutterudite-like CeP_3 at 0 GPa.

Fermi level (E_F) initially increases and then decreases with the presence of $4f$ electrons (Fig. 2), which are bounded by the semifilled $4f$ orbital ($4f^7$). Moreover, the metallic behavior of these compounds is primarily attributed to the presence of M $4f$ electrons, with a minor contribution from M $5d$ and P $3p$ electrons (Fig. S3 [43]). Given that an excess of $4f/5d$ electrons at the E_F is not conducive to superconductivity [50], we have selected metallic CeP_3 , which possesses the fewest $4f/5d$ electrons, as an example to analyze its stability mechanism, electronic properties, and superconducting characteristics. Finally, we also propose a potential synthesis method for this compound. Further discussions on the other compounds are planned for a future detailed study.

To elucidate the interatomic interactions and the stability mechanism of both skutterudite-like and conventional skutterudite-type CeP_3 , we conducted a characterization and comparison of their bonding properties by analyzing the electron localized function (ELF) and the crystal orbital Hamilton population (COHP). In both structures, the P atom exhibits sp^3 hybridization, but the atomic bonds are different. In the conventional skutterudite-type structure, the P atom is bonded to two metal atoms and two other P atoms [51]. In contrast, in skutterudite-like CeP_3 , the P atom forms bonds involving its two lone pair electrons and two adjacent P atoms [Figs. 3(a) and 3(b)]. The calculated COHP reveals that the interaction of the P-P bond within the P_4 ring in the skutterudite-like CeP_3 primarily arises from the hybridized states of P $3s$ with P $3p_x$, and P $3p_z$ with P $3p_x$ orbitals [Fig. 3(b)]. At 0 GPa, the negative integrated COHP ($-\text{ICOHP}$) value is 2.36 eV/pair with a bond distance of 2.30 Å, which is slightly smaller than the $-\text{ICOHP}$ value of 3.00 eV/pair with a bond distance of

2.31 Å in conventional skutterudite-type CeP_3 . Regarding the metal atom, in the conventional skutterudite-type structure, it forms d^2sp^3 hybridized polar covalent bonds with the surrounding six P atoms, characterized by an $-\text{ICOHP}$ value of 1.21 eV/pair and a bond length of 2.91 Å [51]. In contrast, the Ce atom in the skutterudite-like CeP_3 engages in ionic interactions with the surrounding 12 P atoms due to the absence of a clear distribution of electronic states pointing towards the Ce atom [Fig. 3(a)]. This is consistent with a smaller $-\text{ICOHP}$ value of 0.69 eV/pair and a bond distance of 2.98 Å for the Ce-P pair. Consequently, the stability mechanism of skutterudite-like CeP_3 can be attributed to the combined Ce-P interactions and the denser arrangement facilitated by the rotation and distortion of the P_4 ring.

Given that the interesting metallicity observed in skutterudite-like CeP_3 , which involves the Ce $4f$ and P $3p$ electrons [Fig. 4(e)], we delve into its underlying metallic origin. To do this, we initially construct a hypothetical Ce_0P_3 model by removing the Ce atoms from the structure (Fig. S4 [43]). Following the minimum energy principle and considering the bonding environment of the P atom with five valence electrons, two of these electrons form covalent bonds with neighboring P atoms. However, the remaining three electrons reside on the outer side of the P_4 ring as unpaired electrons [Fig. 4(d)]. Ce_0P_3 displays metallic properties owing to the presence of these unpaired electrons. If each P atom were to gain an additional electron, resulting in four unpaired electrons on the outer side (including two lone pair electrons), the compound would satisfy the octet rule and exhibit nonmetallic properties. This is demonstrated in the Ce_0S_3 model, created by substituting P with S atoms (Fig. S5). By combining the observed charge transfer from Ce to P atoms in the qualitative Bader charge analysis with the occupation of antibonding states in the P-P bonds [Fig. 3(b)], we can conclude that the metallicity of CeP_3 primarily arises from multiple charge transfers from Ce to P atoms [Fig. 4(d)]. Specifically, one electron is transferred to the lone pair electrons of the P atom, causing the compound to exhibit nonmetallic properties akin to Ce_0S_3 . Meanwhile, the remaining few electrons are transferred to the antibonding orbital of the P-P bond, which weakens the strength of the P-P bond and enhances electronic connectivity.

Studying the topological structure of Fermi surfaces provides insights into the electronic behavior at the E_F . In skutterudite-like CeP_3 , there are four bands that intersect the E_F [Fig. 4(f)]. However, for the sake of brevity, we will focus on the analysis of band 2, band 3, and band 4, as they make significant contributions to the Fermi surface. Band 2 crosses the E_F along the Γ - M/R and X - R directions, and it exhibits characteristics of both a hole pocket and a steep band. This Fermi surface associated with band 2 has an interesting topology resembling a hollow fire hydrant with a central ball [Fig. 4(a)]. This Fermi surface is primarily attributed to a hybridized state involving Ce $4f_{xz^2}/f_{x(x^2-3y^2)}/f_{z(x^2-y^2)}/f_{y(3x^2-y^2)}$ and P $3p_x$ orbitals (Fig. S7a). Band 3 and band 4 in skutterudite-like CeP_3 exhibit clear degeneracy along the X - R - M and Γ - R directions, and they demonstrate high band dispersion near the E_F . Notably, band 3 also exhibits characteristics of electron pockets along the Γ - M direction. The Fermi surfaces associated with band 3 and

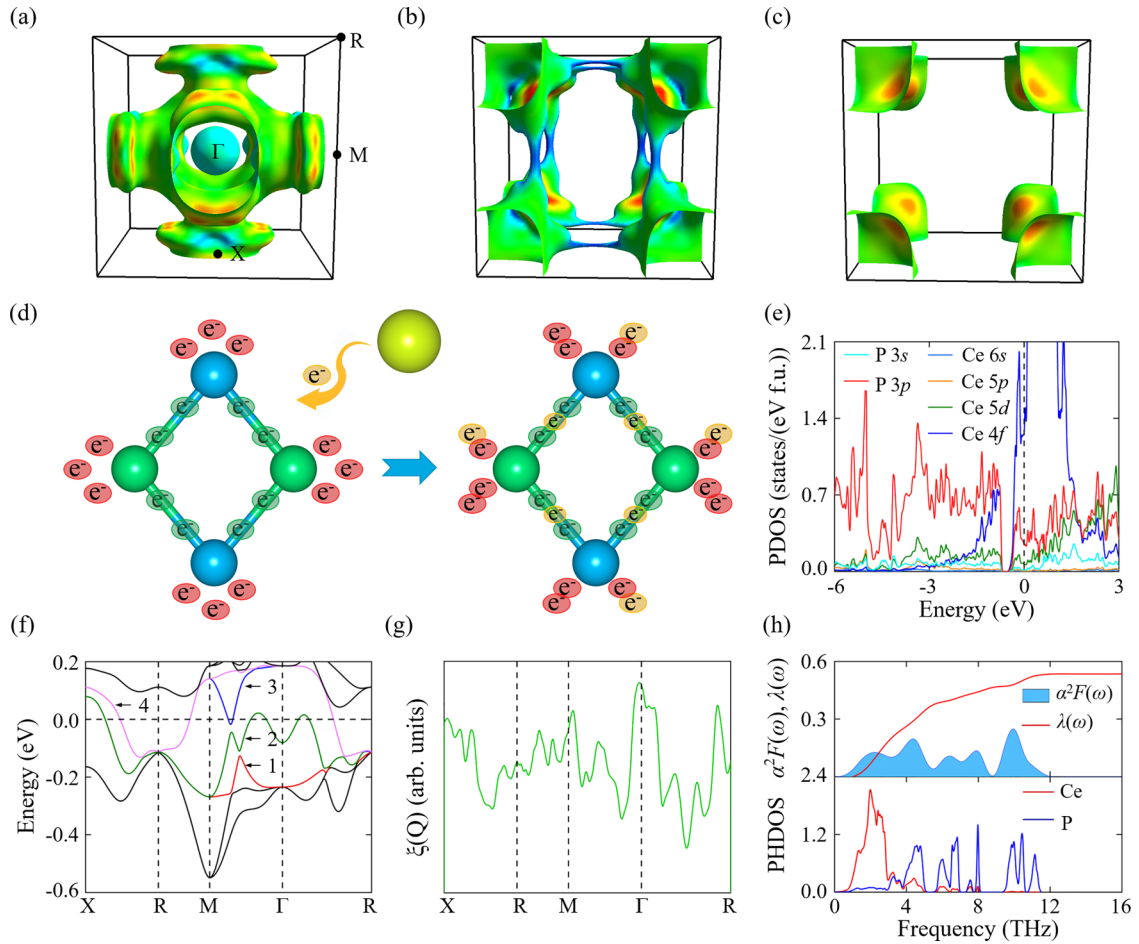


FIG. 4. (a)–(c) The considered three Fermi surfaces (the rest are in Fig. S6 [43]), (d) the schematic diagram of the metallic origin, (e) PDOS, (f) electronic band structure (numbers 1–4 represent the serial number of the band crossing the E_F), (g) the Fermi surface nesting function $\xi(Q)$, and (h) Eliashberg spectral function $\alpha^2F(\omega)$, electron-phonon coupling (EPC) parameter λ , and the projected phonon density of states (PHDOS) of skutterudite-like CeP₃ at 0 GPa.

band 4 can be visualized as consisting of eight interconnected and discrete curved surfaces, oriented towards the Brillouin zone vertices [Figs. 4(b) and 4(c)]. These Fermi surfaces arise from the contribution of Ce $4f_{yz^2}/f_{xz^2}/f_{x(x^2-3y^2)}/f_{z(x^2-y^2)}$ electronic states (Figs. S7b and S7c). It is indeed intriguing that the skutterudite-like CeP₃ structure exhibits Fermi surface nesting behavior along all high-symmetry paths, as indicated by the sharp peaks in the Fermi surface nesting function $\xi(Q)$ [Fig. 4(g)]. These characteristics, including the presence of electron/hole pockets, steep bands, and Fermi surface nesting behavior, have become important indicators of compounds that have the potential to undergo superconducting transitions [52,53].

Based on the Bardeen-Cooper-Schrieffer (BCS) theory, an investigation into the superconducting properties of skutterudite-like CeP₃ at 0 GPa reveals an estimated electron-phonon coupling (EPC) parameter λ of 0.54. This value is comparable to that of several filled skutterudites, such as 0.62 for Ba_{0.89}Ir₄P₁₂ and 0.74 for LaRu₄P₁₂ [54,55]. Upon combining the Eliashberg spectral function $\alpha^2F(\omega)$ with the phonon density of states (PHDOS), it can be concluded that the low-frequency phonon vibrations, associated with the coupling between Ce and P atoms (below 5.5 THz), make a significant

contribution (70%) to the total λ . Conversely, the high-frequency vibrations, primarily originated from the P atoms, contribute only 30% [Fig. 4(h)]. Furthermore, the strong dominance of low-frequency EPC can be attributed to the heavier atomic mass and compact structure of skutterudite-like CeP₃. Consequently, the superconductivity in this material primarily arises from the coupling between low-frequency Ce and P atomic phonons with the Ce $4f$ and P $3p$ electrons. By applying the Allen-Dynes modified McMillan equation, the estimated superconducting transition temperature (T_c) of skutterudite-like CeP₃ is determined to be 2.57 K at 0 GPa with a typical Coulomb pseudopotential μ^* of 0.10 [56,57]. This value is in close agreement with experimental and theoretical values reported for electron/hole doped skutterudites, such as 5.35 K for BaPt₄Ge₁₂ and 6.95 K for LaRu₄P₁₂ at 0 GPa [55,58], and 4.80 K for IrP₃ at 100 GPa [17].

Considering that pressure is an effective strategy for stabilizing unconventional compounds, it is natural to wonder whether the designed skutterudite-like CeP₃ can maintain its thermodynamic and dynamical stability within the high-pressure Ce-P phase diagram. Through first-principles structure search calculations, it has indeed been identified that skutterudite-like CeP₃ remains a stable ground-state structure

even at 25 GPa (Fig. S8). It still maintains superconductivity at 25 GPa, but with a slightly lower T_c of 1.14 K due to the weakened EPC caused by the reduced DOS at the E_F (Table S2 [43]). Furthermore, skutterudite-like CeP_3 exhibits a significant transition potential barrier of 1.53 eV/atom that must be overcome to revert to the conventional skutterudite-type CeP_3 at ambient pressure (Fig. S9). This indicates a strong irreversibility after the rotation of the P_4 units. The energy of formation of skutterudite-like CeP_3 , obtained by combining the most stable precursors CeP and P under ambient pressure, falls within the range of reported metastable phases (<50 meV/atom) (Fig. S10) [49]. Consequently, this rotated skutterudite-like compound holds great potential for synthesis through the process of compressing CeP and P at 25 GPa, and subsequently quenching to ambient pressure. This method has been widely explored in the synthesis of compounds, such as diamond [59], carbides (e.g., BC_3) [60], and nitrides (e.g., PtN_2 [61]), which cannot be obtained under ambient pressure.

IV. CONCLUSIONS

In summary, our study introduces a skutterudite-like structure achieved by rotating the P atomic building blocks within the conventional skutterudite framework. We conducted a comprehensive analysis and identified 14 dynamically stable MP_3 ($M = \text{metal}$) compounds at 0 GPa through first-principles high-throughput screening. Of particular interest is the skutterudite-like CeP_3 , which has been found to be thermodynamically stable at 25 GPa in the Ce-P system, and irreversible at ambient pressure. This indicates its potential synthesis through a compression and subsequent recovery process. Skutterudite-like CeP_3 exhibits metallic properties,

attributed to the excess electrons provided by Ce atoms occupying the antibonding orbitals of the P-P bonds, thereby enhancing electron connectivity. Moreover, skutterudite-like CeP_3 displays an interesting superconductivity with a critical temperature of 2.57 K at 0 GPa. This superconductivity arises from the coupling of Ce/P atomic phonons and the electrons within the $\text{Ce } 4f$ and $\text{P } 3p$ orbitals. Our research provides a strong foundation for the design of superconducting skutterudite-like compounds.

The data that support the findings of this study are available from the corresponding author upon reasonable request.

ACKNOWLEDGMENTS

The authors acknowledge funding from the Natural Science Foundation of China under Grants No. 22372142, No. 12304028, and No. U23A20537, the High-End Foreign Expert Introduction Program (Grant No. G2023003004L), the Central Guiding Local Science and Technology Development Fund Projects (Project No. 236Z7605G), the Natural Science Foundation of Hebei Province (Grant No. B2021203030), and the Science and Technology Project of Hebei Education Department (Grant No. JZX2023020). A.B. acknowledges financial support from the Spanish Ministry of Science and Innovation (Grant No. PID2022-139230NB-I00) and the Department of Education, Universities and Research of the Basque Government and the University of the Basque Country (Grant No. IT1707-22). This work was carried out at the National Supercomputer Center in Tianjin, and the calculations were performed on TianHe-1 (A).

The authors declare no competing financial interest.

-
- [1] X. Gui, B. Lv, and W. Xie, Chemistry in superconductors, *Chem. Rev.* **121**, 2966 (2021).
- [2] M. Lluell, P. Alemany, S. Alvarez, V. P. Zhukov, and A. Vernes, Electronic structure and bonding in skutterudite-type phosphides, *Phys. Rev. B* **53**, 10605 (1996).
- [3] H. Luo, J. W. Krizan, L. Muechler, N. Haldolaarachchige, T. Klimczuk, W. Xie, M. K. Fuccillo, C. Felser, and R. J. Cava, A large family of filled skutterudites stabilized by electron count, *Nat. Commun.* **6**, 6489 (2015).
- [4] G. Cao, P. Liu, S. Zhang, J. Hu, Z. Wang, J. Pan, J. Mao, and G. Shao, Size effect on the electrochemical reaction path and performance of nano size phosphorus rich skutterudite nickel phosphide, *J. Alloys Compd.* **781**, 1059 (2019).
- [5] Z.-Y. Liu, J.-L. Zhu, X. Tong, S. Niu, and W.-Y. Zhao, A review of CoSb_3 -based skutterudite thermoelectric materials, *J. Adv. Ceram.* **9**, 647 (2020).
- [6] R. Hanus, X. Guo, Y. Tang, G. Li, G. J. Snyder, and W. G. Zeier, A chemical understanding of the band convergence in thermoelectric CoSb_3 skutterudites: Influence of electron population, local thermal expansion, and bonding interactions, *Chem. Mater.* **29**, 1156 (2017).
- [7] N. Takeda and M. Ishikawa, Anomalous magnetic properties of $\text{CeRu}_4\text{Sb}_{12}$, *Phys. B (Amsterdam, Neth.)* **259–261**, 92 (1999).
- [8] M. Nicklas, S. Kirchner, R. Borth, R. Gumeniuk, W. Schnelle, H. Rosner, H. Borrmann, A. Leithe-Jasper, Y. Grin, and F. Steglich, Charge-doping-driven evolution of magnetism and non-Fermi-liquid behavior in the filled skutterudite $\text{CePt}_4\text{Ge}_{12-x}\text{Sb}_x$, *Phys. Rev. Lett.* **109**, 236405 (2012).
- [9] Y. Nakanishi, T. Kumagai, M. Oikawa, T. Tanizawa, M. Yoshizawa, H. Sugawara, and H. Sato, Elastic properties of the non-Fermi-liquid metal $\text{CeRu}_4\text{Sb}_{12}$ and dense Kondo semiconductor $\text{CeOs}_4\text{Sb}_{12}$, *Phys. Rev. B* **75**, 134411 (2007).
- [10] X. Lou, T. L. Yu, Y. H. Song, C. H. P. Wen, W. Z. Wei, A. Leithe-Jasper, Z. F. Ding, L. Shu, S. Kirchner, H. C. Xu *et al.*, Distinct Kondo screening behaviors in heavy fermion filled skutterudites with $4f^1$ and $4f^2$ configurations, *Phys. Rev. Lett.* **126**, 136402 (2021).
- [11] S. V. Dordevic, D. N. Basov, N. R. Dilley, E. D. Bauer, and M. B. Maple, Hybridization gap in heavy fermion compounds, *Phys. Rev. Lett.* **86**, 684 (2001).
- [12] M. Imai, M. Arai, and T. Taniguchi, Superconductivity in filled skutterudite $\text{La}_x\text{Rh}_4\text{P}_{12}$ ($0.5 < x \leq 1$): Experimental and computational studies, *Acta Mater.* **166**, 543 (2019).
- [13] R. W. Hill, S. Li, M. B. Maple, and L. Taillefer, Multiband order parameters for the $\text{PrOs}_4\text{Sb}_{12}$ and $\text{PrRu}_4\text{Sb}_{12}$ skutterudite superconductors from thermal conductivity measurements, *Phys. Rev. Lett.* **101**, 237005 (2008).
- [14] M. Rull-Bravo, A. Moure, J. F. Fernández, and M. Martín-González, Skutterudites as thermoelectric materials: Revisited, *RSC Adv.* **5**, 41653 (2015).

- [15] R. Gumeniuk, W. Schnelle, H. Rosner, M. Nicklas, A. Leithe-Jasper, and Y. Grin, Superconductivity in the platinum germanides $M\text{Pt}_4\text{Ge}_{12}$ (M = rare-earth or alkaline-earth metal) with filled skutterudite structure, *Phys. Rev. Lett.* **100**, 017002 (2008).
- [16] Y. Kawamura, S. Deminami, K. Takeda, T. Kuzuya, L. Salamakha, H. Michor, E. Bauer, J. Gouchi, Y. Uwatoko, T. Kawae *et al.*, Crystallographic and superconducting properties of filled skutterudite $\text{SrOs}_4\text{P}_{12}$, *Phys. Rev. B* **103**, 085139 (2021).
- [17] C. Pei, T. Ying, Q. Zhang, X. Wu, T. Yu, Y. Zhao, L. Gao, C. Li, W. Cao, Q. Zhang *et al.*, Caging-Pnictogen-Induced Superconductivity in Skutterudites IrX_3 ($X = \text{As}, \text{P}$), *J. Am. Chem. Soc.* **144**, 6208 (2022).
- [18] Y. Cao, V. Fatemi, S. Fang, K. Watanabe, T. Taniguchi, E. Kaxiras, and P. Jarillo-Herrero, Unconventional superconductivity in magic-angle graphene superlattices, *Nature (London)* **556**, 43 (2018).
- [19] Y. Zhao, X. Zhang, X. Li, S. Ding, Y. Liu, and G. Yang, Emergent superconductivity in K_2ReH_9 under pressure, *J. Mater. Chem. C* **10**, 14626 (2022).
- [20] Y.-M. Kim, A. Kumar, A. Hatt, A. N. Morozovska, A. Tselev, M. D. Biegalski, I. Ivanov, E. A. Eliseev, S. J. Pennycook, J. M. Rondinelli *et al.*, Interplay of octahedral tilts and polar order in BiFeO_3 films, *Adv. Mater.* **25**, 2497 (2013).
- [21] H. Akamatsu, Y. Kumagai, F. Oba, K. Fujita, K. Tanaka, and I. Tanaka, Strong spin-lattice coupling through oxygen octahedral rotation in divalent europium perovskites, *Adv. Funct. Mater.* **23**, 1864 (2013).
- [22] S. Yoshida, H. Akamatsu, A. S. Gibbs, S. Kawaguchi, V. Gopalan, K. Tanaka, and K. Fujita, Interplay between oxygen octahedral rotation and deformation in the acentric ARTiO_4 series toward negative thermal expansion, *Chem. Mater.* **34**, 6492 (2022).
- [23] D. Yi, C. L. Flint, P. P. Balakrishnan, K. Mahalingam, B. Urwin, A. Vailionis, A. T. N'Diaye, P. Shafer, E. Arenholz, Y. Choi *et al.*, Tuning perpendicular magnetic anisotropy by oxygen octahedral rotations in $\text{La}_{1-x}\text{Sr}_x\text{MnO}_3/\text{SrIrO}_3$ superlattices, *Phys. Rev. Lett.* **119**, 077201 (2017).
- [24] Z. Liao, M. Huijben, Z. Zhong, N. Gauquelin, S. Macke, R. J. Green, S. Van Aert, J. Verbeeck, G. Van Tendeloo, K. Held *et al.*, Controlled lateral anisotropy in correlated manganite heterostructures by interface-engineered oxygen octahedral coupling, *Nat. Mater.* **15**, 425 (2016).
- [25] Y. Cao, V. Fatemi, A. Demir, S. Fang, S. L. Tomarken, J. Y. Luo, J. D. Sanchez-Yamagishi, K. Watanabe, T. Taniguchi, and E. Kaxiras, Correlated insulator behaviour at half-filling in magic-angle graphene superlattices, *Nature (London)* **556**, 80 (2018).
- [26] F. Lavini, M. Rejhon, and E. Riedo, Two-dimensional diamonds from sp^2 -to- sp^3 phase transitions, *Nat. Rev. Mater.* **7**, 814 (2022).
- [27] Z. Zhao, S. Zhang, T. Yu, H. Xu, A. Bergara, and G. Yang, Predicted pressure-induced superconducting transition in electride Li_6P , *Phys. Rev. Lett.* **122**, 097002 (2019).
- [28] L. Zhu, G. M. Borstad, H. Liu, P. A. Guñka, M. Guerette, J.-A. Dolyniuk, Y. Meng, E. Greenberg, V. B. Prakapenka, B. L. Chaloux *et al.*, Carbon-boron clathrates as a new class of sp^3 -bonded framework materials, *Sci. Adv.* **6**, eaay8361 (2020).
- [29] D. Duan, Y. Liu, F. Tian, D. Li, X. Huang, Z. Zhao, H. Yu, B. Liu, W. Tian, and T. Cui, Pressure-induced metallization of dense $(\text{H}_2\text{S})_2\text{H}_2$ with high- T_c superconductivity, *Sci. Rep.* **4**, 6968 (2014).
- [30] H. Liu, I. I. Naumov, R. Hoffmann, N. W. Ashcroft, and R. J. Hemley, Potential high- T_c superconducting lanthanum and yttrium hydrides at high pressure, *Proc. Natl. Acad. Sci. U.S.A.* **114**, 6990 (2017).
- [31] J.-N. Wang, X.-W. Yan, and M. Gao, High-temperature superconductivity in SrB_3C_3 and BaB_3C_3 predicted from first-principles anisotropic Migdal-Eliashberg theory, *Phys. Rev. B* **103**, 144515 (2021).
- [32] W. Chen, D. V. Semenok, X. Huang, H. Shu, X. Li, D. Duan, T. Cui, and A. R. Oganov, High-temperature superconducting phases in cerium superhydride with a T_c up to 115 K below a pressure of 1 Megabar, *Phys. Rev. Lett.* **127**, 117001 (2021).
- [33] K. Momma and F. Izumi, VESTA3 for three-dimensional visualization of crystal, volumetric and morphology data, *J. Appl. Crystallogr.* **44**, 1272 (2011).
- [34] J. Hafner, Ab-initio simulations of materials using VASP: Density-functional theory and beyond, *J. Comput. Chem.* **29**, 2044 (2008).
- [35] S. Baroni, S. de Gironcoli, A. Dal Corso, and P. Giannozzi, Phonons and related crystal properties from density-functional perturbation theory, *Rev. Mod. Phys.* **73**, 515 (2001).
- [36] P. E. Blöchl, Projector augmented-wave method, *Phys. Rev. B* **50**, 17953 (1994).
- [37] J. P. Perdew, J. A. Chevary, S. H. Vosko, K. A. Jackson, M. R. Pederson, D. J. Singh, and C. Fiolhais, Atoms, molecules, solids, and surfaces: Applications of the generalized gradient approximation for exchange and correlation, *Phys. Rev. B* **46**, 6671 (1992).
- [38] G.-R. Qian, X. Dong, X.-F. Zhou, Y. Tian, A. R. Oganov, and H.-T. Wang, Variable cell nudged elastic band method for finding solid-solid structural phase transitions, *Comput. Phys. Commun.* **184**, 2111 (2013).
- [39] C. W. Glass, A. R. Oganov, and N. Hansen, USPEX—Evolutionary crystal structure prediction, *Comput. Phys. Commun.* **175**, 713 (2006).
- [40] A. D. Becke and K. E. Edgecombe, A simple measure of electron localization in atomic and molecular systems, *J. Chem. Phys.* **92**, 5397 (1990).
- [41] R. Nelson, C. Ertural, J. George, V. L. Deringer, G. Hautier, and R. Dronskowski, LOBSTER: Local orbital projections, atomic charges, and chemical-bonding analysis from projector-augmented-wave-based density-functional theory, *J. Comput. Chem.* **41**, 1931 (2020).
- [42] P. Giannozzi, S. Baroni, N. Bonini, M. Calandra, R. Car, C. Cavazzoni, D. Ceresoli, G. L. Chiarotti, M. Cococcioni, I. Dabo *et al.*, QUANTUM ESPRESSO: A modular and open-source software project for quantum simulations of materials, *J. Phys.: Condens. Matter* **21**, 395502 (2009).
- [43] See Supplemental Material at <http://link.aps.org/supplemental/10.1103/PhysRevB.109.054522> for computational details; electronic band structures of the skutterudite-like YP_3/LaP_3 ; structural information and relative enthalpies of skutterudite-like CeP_3 at 0 GPa; transition barrier required to revert the skutterudite-like CeP_3 to the classical skutterudite-type CeP_3 at 0 GPa; convex hull of Ce-P compounds at 25 GPa. The Supplemental Material also contains Refs. [41,42,44–49].

- [44] Y. Wang, J. Lv, L. Zhu, and Y. Ma, Crystal structure prediction via particle-swarm optimization, *Phys. Rev. B* **82**, 094116 (2010).
- [45] Y. Wang, J. Lv, L. Zhu, and Y. Ma, CALYPSO: A method for crystal structure prediction, *Comput. Phys. Commun.* **183**, 2063 (2012).
- [46] P. B. Allen and R. C. Dynes, Transition temperature of strongly-coupled superconductors reanalyzed, *Phys. Rev. B* **12**, 905 (1975).
- [47] J. P. Carbotte, Properties of boson-exchange superconductors, *Rev. Mod. Phys.* **62**, 1027 (1990).
- [48] P. B. Allen and B. Mitrović, Theory of Superconducting T_c , *Solid State Phys.* **37**, 1 (1983).
- [49] Y. Hinuma, T. Hatakeyama, Y. Kumagai, L. A. Burton, H. Sato, Y. Muraba, S. Iimura, H. Hiramatsu, I. Tanaka, H. Hosono *et al.*, Discovery of earth-abundant nitride semiconductors by computational screening and high-pressure synthesis, *Nat. Commun.* **7**, 11962 (2016).
- [50] D. V. Semenov, I. A. Kruglov, I. A. Savkin, A. G. Kvashnin, and A. R. Oganov, On distribution of superconductivity in metal hydrides, *Curr. Opin. Solid State Mater. Sci.* **24**, 100808 (2020).
- [51] C. Uher, Chapter 5 Skutterudites: Prospective novel thermoelectrics, in *Semiconductors and Semimetals*, edited by T. M. Tritt (Elsevier, New York, 2001), Vol. 69, pp. 139–253.
- [52] A. Simon, Superconductivity and chemistry, *Angew. Chem., Int. Ed. Engl.* **36**, 1788 (1997).
- [53] Z. S. Pereira, G. M. Faccin, and E. Z. da Silva, Predicted superconductivity in the electride Li_5C , *J. Phys. Chem. C* **125**, 8899 (2021).
- [54] Y. Qi, H. Lei, J. Guo, W. Shi, B. Yan, C. Felser, and H. Hosono, Superconductivity in Alkaline Earth Metal-Filled Skutterudites $\text{Ba}_x\text{Ir}_4\text{X}_{12}$ ($X = \text{As}, \text{P}$), *J. Am. Chem. Soc.* **139**, 8106 (2017).
- [55] H. M. Tütüncü, E. Karaca, and G. P. Srivastava, Electron-phonon superconductivity in the filled skutterudites $\text{LaRu}_4\text{P}_{12}$, $\text{LaRu}_4\text{As}_{12}$, and $\text{LaPt}_4\text{Ge}_{12}$, *Phys. Rev. B* **95**, 214514 (2017).
- [56] P. Morel and P. W. Anderson, Calculation of the Superconducting State Parameters with Retarded Electron-Phonon Interaction, *Phys. Rev.* **125**, 1263 (1962).
- [57] A. Sanna, J. A. Flores-Livas, A. Davydov, G. Profeta, K. Dewhurst, S. Sharma, and E. K. U. Gross, Ab initio Eliashberg Theory: Making Genuine Predictions of Superconducting Features, *J. Phys. Soc. Jpn.* **87**, 041012 (2018).
- [58] E. Bauer, A. Grytsiv, X.-Q. Chen, N. Melnychenko-Koblyuk, G. Hilscher, H. Kaldarar, H. Michor, E. Royanian, G. Giester, M. Rotter *et al.*, Superconductivity in novel Ge-based skutterudites: $\{\text{Sr}, \text{Ba}\}\text{Pt}_4\text{Ge}_{12}$, *Phys. Rev. Lett.* **99**, 217001 (2007).
- [59] K. Luo, B. Liu, W. Hu, X. Dong, Y. Wang, Q. Huang, Y. Gao, L. Sun, Z. Zhao, Y. Wu *et al.*, Coherent interfaces govern direct transformation from graphite to diamond, *Nature (London)* **607**, 486 (2022).
- [60] P. V. Zinin, L. C. Ming, H. A. Ishii, R. Jia, T. Acosta, and E. Hellebrand, Phase transition in BC_x system under high-pressure and high-temperature: Synthesis of cubic dense BC_3 nanostructured phase, *J. Appl. Phys.* **111**, 114905 (2012).
- [61] J. C. Crowhurst, A. F. Goncharov, B. Sadigh, C. L. Evans, P. G. Morrall, J. L. Ferreira, and A. J. Nelson, Synthesis and characterization of the nitrides of platinum and iridium, *Science* **311**, 1275 (2006).